The Journal of Experimental Biology 207, 755-765
Published by The Company of Biologists 2004
doi:10.1242/jeb.00810

Why is it worth flying at dusk for aquatic insects? Polarotactic water detection is easiest at low solar elevations

Balázs Bernáth[1,2], József Gál[3] and Gábor Horváth[1,*]

[1]*Biooptics Laboratory, Department of Biological Physics, Eötvös University, H-1117 Budapest, Pázmány sétány 1, Hungary,* [2]*Plant Protection Institute of the Hungarian Academy of Sciences, Department of Zoology, H-1525 Budapest, P. O. B. 102, Hungary* and [3]*International University Bremen IUB, School of Engineering and Science, P. O. B. 750561, D-28725 Bremen-Grohn, Germany*

*Author for correspondence (e-mail: gh@arago.elte.hu)

Accepted 20 November 2003

Summary

Using 180° field-of-view imaging polarimetry, we measured the reflection-polarization patterns of two artificial surfaces (water-dummies) in the red, green and blue spectral ranges under clear and partly cloudy skies at different solar elevations. The dummies consisted of a horizontal glass pane with a matt black or matt light grey cloth underneath, imitating a dark or bright water body, respectively. Assuming that polarotactic water insects interpret a surface as representing water if the degree of linear polarization of reflected light is higher than a threshold and the deviation of the direction of polarization from the horizontal is lower than a threshold, we calculated the proportion, *P*, of the artificial surfaces detected polarotactically as water. We found that at sunrise and sunset *P* is maximal for both water-dummies and their reflection-polarizational characteristics are most similar. From this, we conclude that polarotactic water detection is easiest at low solar elevations, because the risk that a polarotactic insect will be unable to recognize the surface of a dark or bright water body is minimal. This partly explains why many aquatic insect species usually fly *en masse* at dusk. The daily change in the reflection-polarization pattern of water surfaces is an important visual ecological factor that may contribute to the preference of the twilight period for habitat searching by polarotactic water insects. Air temperature at sunrise is generally low, so dusk is the optimal period for polarotactic aquatic insects to seek new habitats.

Key words: dusk-flying water insects, aquatic habitat recognition, polarotaxis, reflection polarization, polarization sensitivity, 180° field-of-view imaging polarimetry.

Introduction

It is a well-documented phenomenon that many aquatic insect species, especially small-bodied Heteroptera (e.g. *Sigara*, *Corixa* and *Cymatia* sp.) but also some Coleoptera (e.g. *Berosus* sp.), seek new habitats during their migration and dispersal *en masse* usually between dusk and midnight (e.g. Popham, 1964; Danilevskii, 1965; Johnson, 1969; Fernando and Galbraith, 1973; Zalom et al., 1979, 1980; Danthanarayana, 1986). From an ecological point of view, this is explained conventionally by the reduced risk of both predation and dehydration as well as by the period of calm and lower air temperature at twilight (e.g. Landin, 1968; Landin and Stark, 1973). At sunset, the intensity of ambient light decreases rapidly, rendering the visual detection of flying prey by birds more difficult (e.g. King and Wrubleski, 1998). Since the rate of dehydration is proportional to the surface-to-volume ratio, small-bodied aquatic insects become easily dehydrated during flight if they cannot find a body of water within ~1 h. At nightfall, the lower temperature, higher relative humidity and calmness of air relative to those in daytime are optimal for small-bodied aquatic insects (Landin and Stark, 1973).

The aim of the present study is to show that the daily change in the reflection-polarization pattern of water surfaces is a further important visual ecological factor that may contribute to the preference for the twilight period for habitat searching by polarotactic water insects. These insects detect water by means of the horizontal polarization of light reflected from the water surface (Schwind, 1991, 1995; Horváth and Varjú, 2003). Using 180° field-of-view imaging polarimetry, we measured the reflection-polarization patterns of two artificial surfaces (water-dummies) in the red, green and blue spectral ranges under clear and partly cloudy skies at different solar elevations. The water-dummies were composed of a horizontal glass pane underneath which was a matt black or a matt light grey cloth, which imitated a dark or bright water body, respectively.

Assuming that polarotactic water insects interpret a surface to be water if the degree of linear polarization of reflected light is higher than a threshold and the deviation of the direction of polarization from the horizontal is lower than a threshold, we calculated the proportion, *P*, of the dummy surface detected polarotactically as water. We found that at sunrise and sunset *P* is maximal for both water-dummies, and at these times their

reflection-polarizational characteristics are most similar. From this, we conclude that polarotactic water detection is easiest at low solar elevations, because the risk that a polarotactic insect will be unable to recognize the surface of a dark or bright water body is minimal. This partly explains why many aquatic insect species usually fly *en masse* at dusk. As the air temperature at sunrise is generally too low, dusk is the optimal period for polarotactic aquatic insects to seek new habitats.

The results presented here could be achieved using the 180° field-of-view imaging polarimetry developed recently by Gál et al. (2001a,b) and Horváth et al. (2002), with which the full polarization pattern of horizontal reflecting surfaces can be measured. This technique made it possible to measure the *P*-values of polarizing surfaces in the entire lower hemispherical visual field of a hypothetical flying polarotactic water insect. Previously, such measurements and the derivation of *P* could not be performed, because earlier imaging polarimetric measurements (e.g. Horváth and Zeil, 1996; Horváth and Varjú, 1997; Horváth et al., 1997, 1998; Kriska et al., 1998; Bernáth et al., 2002) were restricted to relatively small (~40°×50° maximum) fields of view.

Materials and methods

Originally, we planned to measure the reflection-polarization pattern of water surfaces by means of 180° field-of-view imaging polarimetry. The calibration of this technique and the evaluation of the photographs are described in detail by Gál et al. (2001a,b) and Horváth et al. (2002). Since our down-facing polarimeter must be suspended somehow above the water surface, which must not undulate during recording, it would be enormously difficult to perform such measurements above water surfaces over a period of time (Fig. 1A). The requirement for a cloudless sky and no wind to ensure flat water surfaces can be met only by chance (Gál et al., 2001a). This makes such comparative polarimetric measurements almost impossible throughout the day. Thus, we subsequently decided to use water-imitating artificial reflecting surfaces called ‘water-dummies’.

One of the water-dummies consisted of a horizontal glass pane (1 m×1 m) underlaid by a piece of plywood covered with a matt black cloth. This imitated either a dark water body (with transparent water and a black bottom) or deep water (from which only a small amount of light is returned from the subsurface layers). The other water-dummy was a horizontal glass pane (1 m×1 m) underlaid with a piece of plywood covered by a matt light grey cloth, which mimicked either a bright water body (with transparent, shallow water and a bright bottom) or a water body with bright suspended particles (from which a considerable amount of light is returned in comparison with the amount of surface-reflected light). The water-dummies were laid horizontally on levelled metal holders 30 cm above the ground (Fig. 1A) on a hill top in order to minimise the disturbing mirroring of landmarks near the horizon. The horizontality of the dummies was checked by water levels. The relative reflectivity of the black and grey cloths and the water-dummies (Fig. 1B) *versus* the wavelength was measured with a Jobin Yvon-Spex Fluoromax-2 spectrofluorimeter (Jobin Yvon Ltd, Edison, NJ, USA). We showed that the conclusions drawn from the data obtained for the glass water-dummies also hold for flat water surfaces. Similar dummies with manipulated reflection-polarizational and spectral characteristics were successfully applied by Schwind (1991, 1995) to study the polarotaxis of water insects.

Our imaging polarimeter was a Nikon F801 photographic camera equipped with a Nikon-Nikkor fisheye lens with a 180° field of view, 8 mm focal length and 2.8 f-number. Fujichrome Sensia II 100 ASA colour reversal films were used as a detector. The fisheye lens possessed a filter wheel with linearly polarizing (HNP’B, Polaroid) filters with three different directions of the transmission axes. With this technique, polarization patterns can be measured in the red (650±30 nm, wavelength of sensitivity maximum ± half bandwidth), green (550±30 nm) and blue (450±50 nm) spectral ranges.

The polarimeter with down-facing fisheye lens was suspended on a holder above the centre of the water-dummy in such a way that the vertical optical axis of the lens pointed towards the nadir (Fig. 1A). In order to minimise the disturbance of the shadow of the holder on the dummy surface, different holder orientations relative to magnetic north were chosen (Fig. 1C). The distance between the outermost surface of the fisheye lens and the glass surface was as small as possible (7 cm) in order to measure the reflection-polarizational characteristics of the water-dummies in a conical field of view as wide as possible (~160°). The fisheye lens was focused into infinity to record the mirror image of the sky reflected from the glass surface. For a complete measurement, three photographs were taken through the polarizers with three different transmission axes. This took ~10 s, during which the operator triggered the expositions by a remote cord and turned the filter wheel of the polarimeter three times. During measurements, the operator lay on the ground below the level of the glass pane to avoid unwanted reflections (Fig. 1A). After the measurement of a water-dummy, it was replaced by the other dummy within ~1 min and the procedure was repeated. This allowed us to measure the reflection-polarization patterns of both dummies within a few minutes, i.e. under almost the same illumination conditions and at the same solar elevation (θ_s).

Measurements were carried out near the time of the summer solstice under sunny, partly cloudy skies on 17 July 2002 and under sunny, cloudless clear skies on 18 July 2002 near Kunfehértó in Hungary (46°23′ N, 19°24′ E) from sunrise (04:49 h; local summer time = Universal Time Conversion + 2 h) to an hour after sunset (20:37 h) at the different θ_s shown in Fig. 1C. The maximum θ_s was 67° at noon (12:56 h). Because of disturbance by early morning dewfall, reflection-polarization patterns at low solar elevations are presented here only for the sunset and dusk period.

The evaluated reflection-polarization patterns are presented here in the form of circular maps, the centre and perimeter of which are the nadir and the horizon, respectively. The

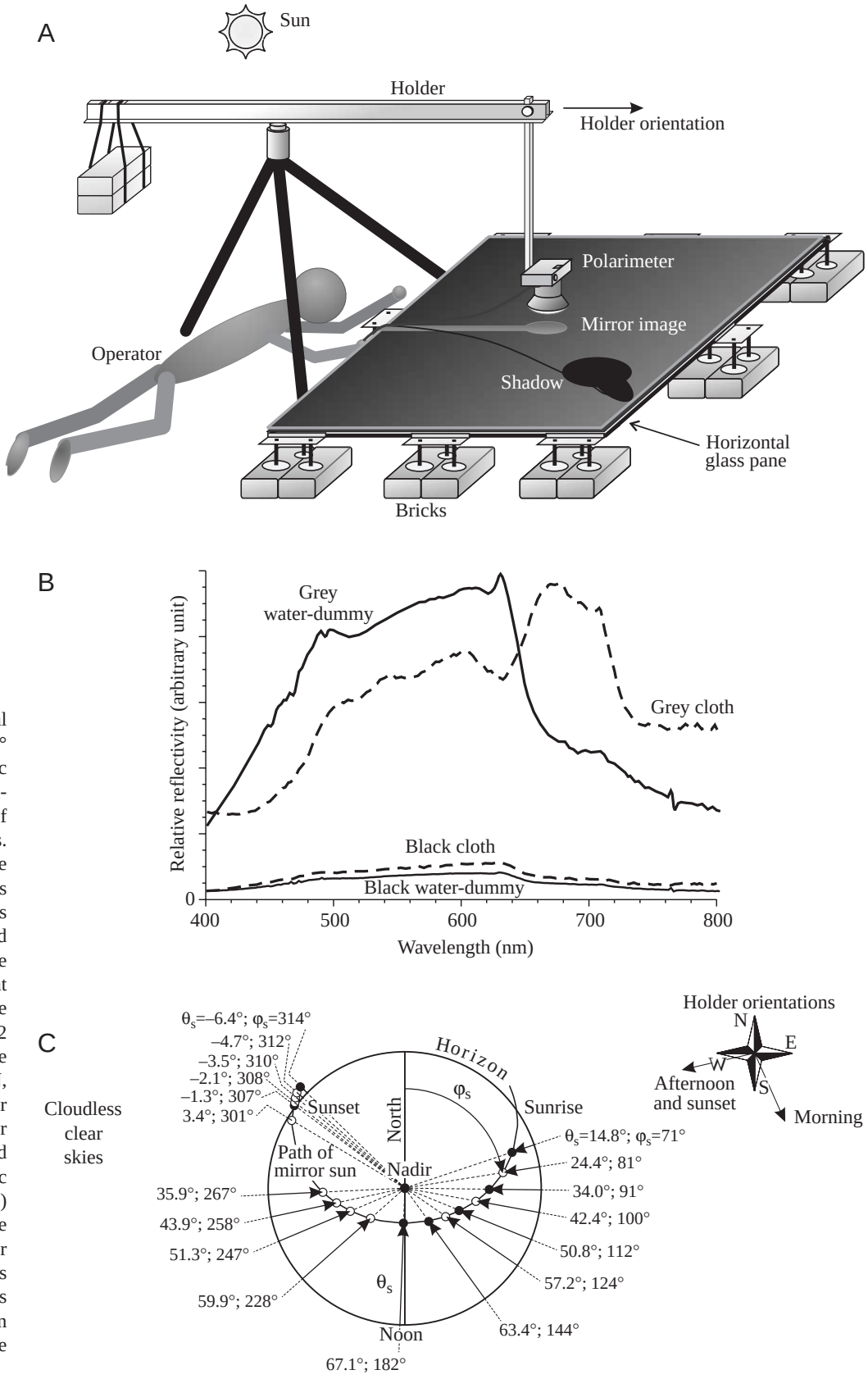

Fig. 1. (A) Experimental arrangement of the 180° field-of-view imaging polarimetric measurement of the reflection-polarizational characteristics of horizontal water-dummies. (B) Relative reflectivities of the matt black and matt grey cloths (used as substrata of the glass panes) as well as the black and grey water-dummies. (C) The mirror image of the apparent celestial path of the sun during the measurements on 18 July 2002 under clear, cloudless skies at the Hungarian Kunfehértó (46°23′ N, 19°24′ E) in a system of polar coordinates, where the solar azimuth angle (φ_s) is measured clockwise from the magnetic north, and the solar elevation (θ_s) is measured radially from the horizon. Dots show the solar positions when the measurements were performed. Black dots represent the solar positions when the patterns in Figs 2 and 3 were measured.

numerical values of the degree (d) and angle (α) of linear polarization are coded by different shades of grey and colours. In these maps, the water-dummies cover an approximately circular area as wide as ~160°. The azimuth angle (φ) of a given direction of view is measured clockwise from the solar meridian, and its nadir angle (ν) is measured radially in such a way, that ν is proportional to the radius (nadir: ν=0°, horizon: ν=90°). Note that the polar system of coordinates used for the representation of the reflection-polarization patterns is simply the mirror image of the celestial polar system of coordinates. Although during measurements the direction of the polarimeter holder relative to the fixed dummies changed as the sun moved along its celestial arc (Fig. 1C), for the sake of a better visualization in Figs 2–4 we present all circular pictures rotated in such a way that the actual solar meridian always points vertically upwards, since these patterns are symmetrical to the solar–antisolar meridian under clear skies.

The mirror image of the polarimeter, its holder and the remote cord, as well as their shadows (Fig. 1A), moved counter-clockwise with respect to the solar meridian over time (Figs 2, 3). Our aim was to compare the reflection-polarization patterns of the two water-dummies. Therefore, for comparative analyses, we excluded regions (chequered in Figs 2, 3) in which landscape near the horizon, unwanted overexposure, disturbing shadows or mirror images of the polarimeter, its holder and remote cord occurred in the individual pictures taken at a given θ_s. Thus, for both dummies at a particular θ_s, we obtained a time-dependent mask, the area of which was inappropriate for comparative analyses and from which viewing directions were not taken into account. Hence, in comparative analyses, only those viewing directions were considered where the mirror image of the sky and the polarizational characteristics of the reflected skylight could be registered without any disturbance.

The reflection-polarization patterns of a perfectly black water-dummy (Fig. 4), absorbing the penetrating component of incident light, were calculated with the mathematical method developed by Schwind and Horváth (1993), Horváth (1995) and Gál et al. (2001a) for incident single-scattered Rayleigh skylight.

Schwind (1985) showed that backswimmers (*Notonecta glauca*) avoid a light source emitting vertically polarized light. The same was demonstrated in dragonflies (Horváth et al., 1998; Wildermuth, 1998), mayflies and many other water-loving insects (Schwind, 1991, 1995; Kriska et al., 1998; Bernáth et al., 2001b). Polarotactic water insects consider any surface as water if (1) the degree of linear polarization of reflected light (d) is higher than the threshold of polarization sensitivity (d_{tr}) and (2) the deviation of the angle of polarization of reflected light from the horizontal ($\Delta\alpha$) is smaller than a threshold ($\Delta\alpha_{tr}$) in that part of the spectrum in which the polarization of reflected light is perceived. Therefore, an imaginary polarotactic water insect levitating above the centre of our water-dummies was assumed to interpret as water those areas of the dummies from which skylight is reflected with the following two criteria: (1) $d>d_{tr}$=5% and (2) $|\alpha-90°|<\Delta\alpha_{tr}$=5°. We introduce the quantity 'percentage P of a reflecting surface detected as water', which is the angular proportion, P, of the viewing directions (relative to the angular extension of 2π steradians of the whole lower hemisphere of the field of view of the insect) for which both criteria are satisfied. In other words, P gives the relative proportion of the entire ventral field of view in which the water-dummies are considered polarotactically to be water. The higher the P-value for a reflecting surface in a given visual environment, the larger its polarotactic detectability; i.e. the higher the probability that a water-seeking insect can find it by polarotaxis. Thus, for the sake of simplicity, P is subsequently called 'polarotactic detectability'. Using the Mann–Whitney test and the statistical program SPSS (version 9.0), the P-values calculated for the grey water-dummy were compared with those of the black dummy in the blue, green and red parts of the spectrum.

Results

Column 1 in Figs 2 and 3 shows the colour photographs (without polarizers) of the mirror image of the clear sky reflected from the grey and black water-dummies, respectively, as a function of θ_s. Since these colour photographs were taken with different times of exposure, they do not display correctly the relative intensity of reflected light. Nevertheless, it is clear that the light reflected from the glass surface dominates relative to the cloth-reflected light at the black water-dummy (Fig. 3), while at the grey dummy (Fig. 2) the cloth-reflected component also contributes significantly to the net amount of returned light.

Column 2 in Figs 2 and 3 shows the patterns of the degree of linear polarization (d) of skylight reflected from the water-dummies in the blue part of the spectrum at different solar elevations. The grey water-dummy is less polarizing than the black one. The light reflected from it is almost unpolarized in many directions of view, and its maximum d is only ~30%. At the Brewster angle – at which the surface-reflected light is totally and horizontally polarized (56° from the nadir for glass) – very low d-values occur in many azimuth angles (Fig. 2). The black water-dummy is an effective polarizer, reflecting highly polarized skylight from many directions of view. At the Brewster angle, a continuous annular region, subsequently called the 'Brewster zone', occurs with maximum d. Depending on θ_s, two neutral points with unpolarized reflected skylight appear within the Brewster zone perpendicular to the solar meridian (Fig. 3).

Column 3 in Figs 2 and 3 shows the patterns of the angle of polarization (α) of skylight reflected from the water-dummies in the blue part of the spectrum. For the grey dummy, as the solar elevation increases, the proportion of the nearly vertically polarized reflected skylight with $-45°<\alpha<45°$ (shown in red and yellow) becomes dominant over the nearly horizontally polarized reflected skylight with $45°<\alpha<135°$ (shown in green and blue) perpendicular to the solar meridian. However, from regions of the grey water-dummy towards the mirror image of

the sun, approximately horizontally polarized light is always reflected. At near-zero solar elevations, this is also the case for regions towards the mirror image of the antisun. From the Brewster zone of the grey dummy, nearly vertically polarized light is always reflected perpendicular to the solar meridian (Fig. 2). From the black water-dummy, predominantly nearly horizontally polarized skylight is always reflected irrespective of θ_s. However, approximately vertically polarized skylight is reflected from 8-shaped regions with long axes perpendicular to the solar–antisolar meridian within the Brewster zone as well as from crescent-shaped areas near the horizon perpendicularly to the solar meridian. From the Brewster zone of the black dummy, horizontally polarized skylight is always reflected (Fig. 3). Note that the mirror images of the polarimeter, its holder and remote cord disturb the α-patterns only slightly. Therefore, in these regions, we omitted the chequered pattern of these mirror images in the

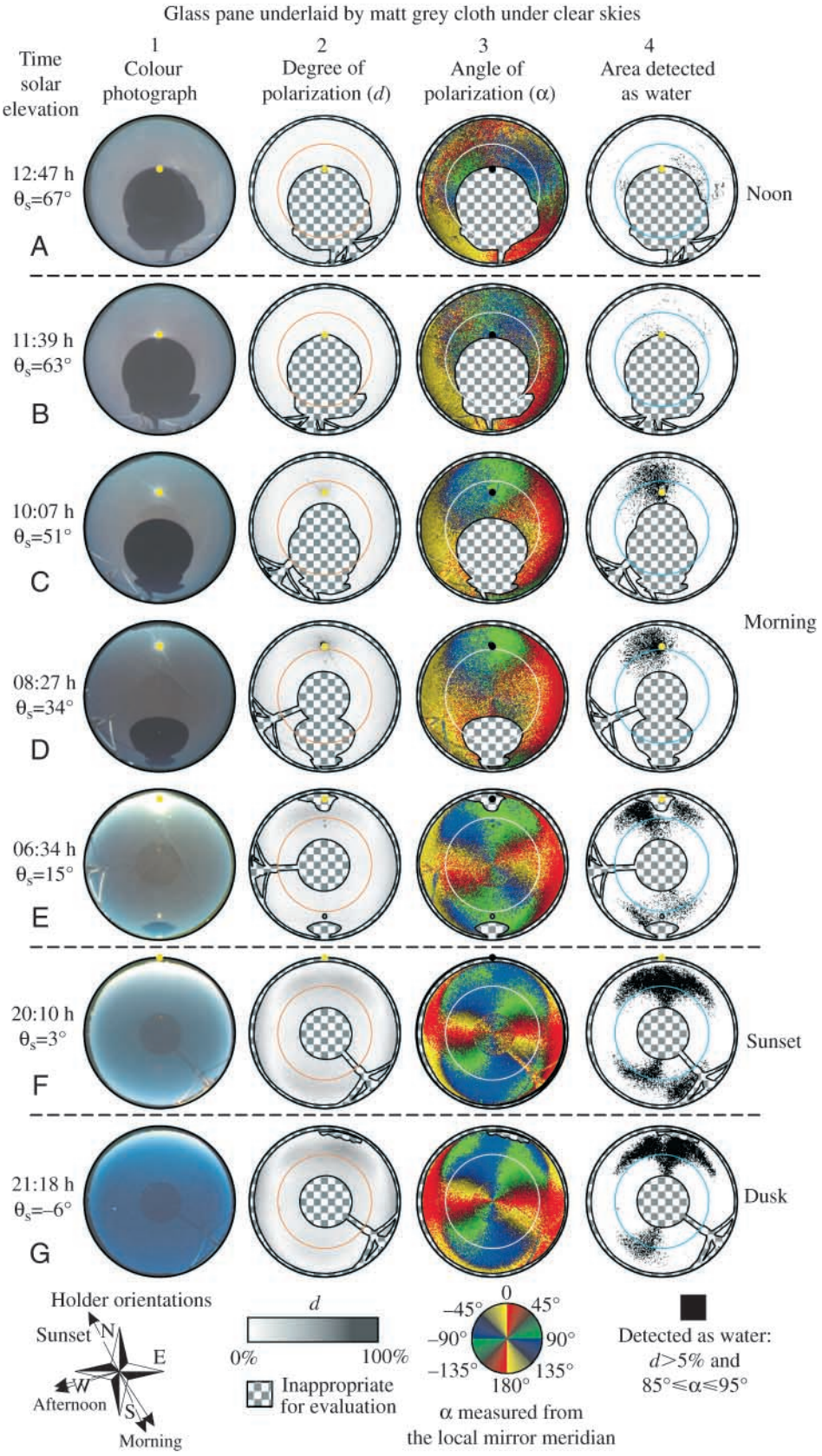

Fig. 2. Colour photographs (without polarizers) of the mirror image of the clear sky reflected from the grey water-dummy (glass pane underlaid by matt light grey cloth), patterns of the degree (d) and angle (α; measured from the local mirror meridian) of linear polarization of reflected skylight, and the area detected polarotactically as water *versus* the solar elevation (θ_s) and time (local solar time = UTC + 2 h). The polarization patterns are measured by 180° field-of-view imaging polarimetry in the blue part of the spectrum. Chequered areas show those regions that are inappropriate for comparative analyses due to unwanted overexposure, shadows and mirror images of the polarimeter, its holder and remote cord. In column 4, regions are shaded by black where $d>d_{tr}=5\%$ and $85°\leq\alpha\leq95°$. An imaginary polarotactic water insect is assumed to consider a surface as water if these two conditions are satisfied for the partially linearly polarized reflected light. In column 4, the regions where these criteria are not satisfied remain blank. The positions of the mirror image of the sun are shown by dots, and the Brewster angle (56° from the nadir for glass with an index of refraction of 1.5) is represented by an inner circle within the circular patterns. Because of disturbance by early morning dewfall, reflection-polarization patterns at low solar elevations are presented here only for the sunset and dusk period.

α-maps of Figs 2 and 3. These regions were, however, not taken into account in comparative analyses.

In column 4 of Figs 2 and 3, the regions of the water-dummies where the degree of polarization $d>d_{tr}=5\%$ and the angle of polarization $|\alpha-90°|<\Delta\alpha_{tr}=5°$ are shaded in black, assuming that the imaginary polarotactic insect detects the water in the blue part of the spectrum. At a solar elevation of 0°, the grey water-dummy is interpreted as water only in areas towards the mirror sun and mirror antisun and partly in the Brewster zone. As θ_s increases, the area detected as water gradually decreases and the grey dummy is considered as water only in small spots around the mirror sun and opposite to it. At higher θ_s, the grey dummy is not interpreted as water even in the Brewster zone (Fig. 2). The black water-dummy is always considered as water at or near the Brewster angle. However, further away from the Brewster angle the black dummy is not interpreted as water perpendicular to the solar meridian (Fig. 3). Since quite similar patterns were obtained in the green and red parts of the spectrum, we omit to present them here.

Fig. 4 shows the patterns of the degree and angle of linear polarization and the areas detected as water for a perfectly black glass reflector (index of refraction $n_g=1.5$) – which absorbs all penetrating light – computed for the same solar elevations as in Figs 2 and 3 and for incident single-scattered Rayleigh skylight. The patterns in Fig. 4 are very similar to those in Fig. 3. Hence, the reflection-polarizational characteristics of the black water-dummy approximate those of a perfectly black glass reflector. The same patterns were also

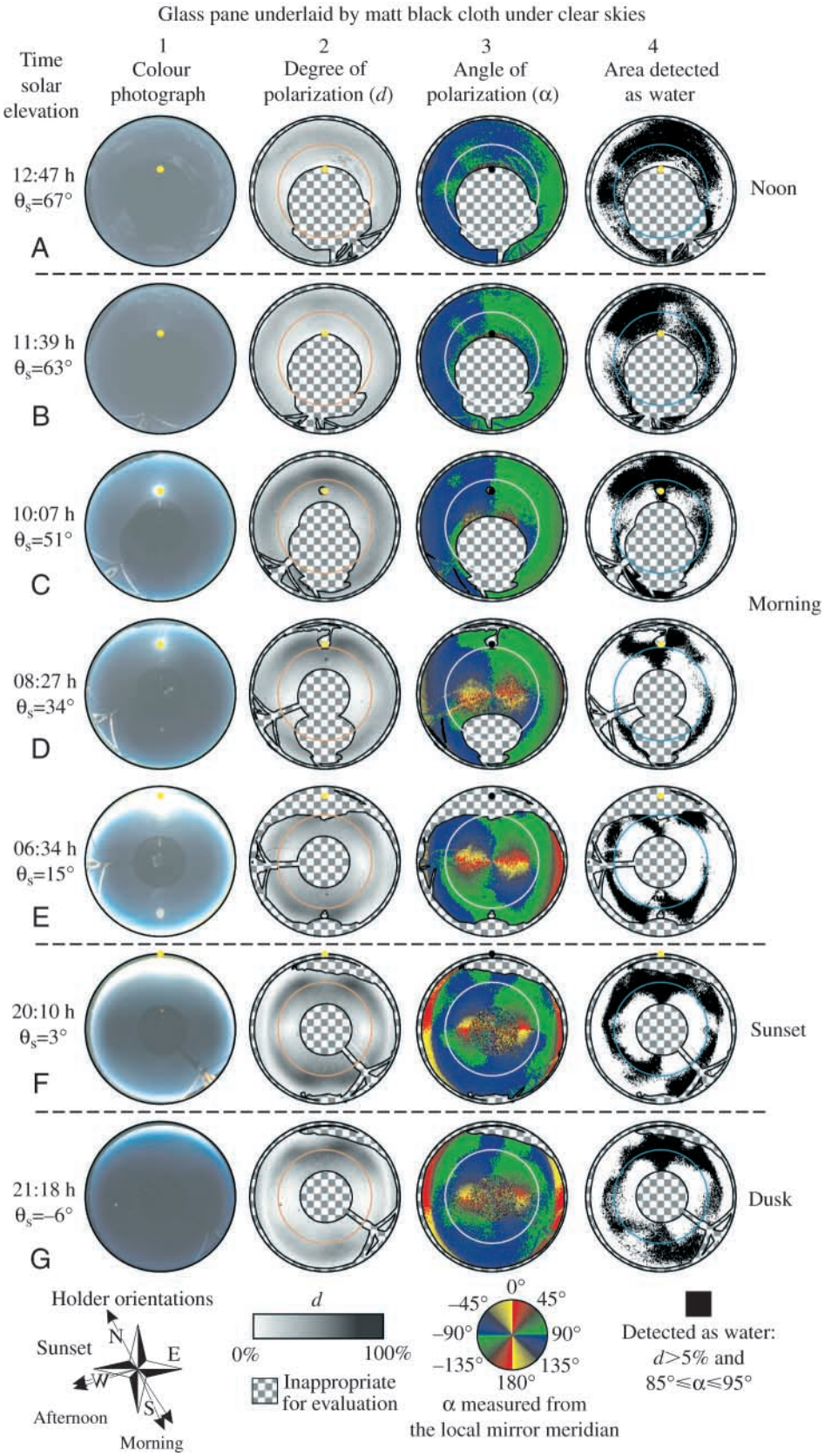

Fig. 3. Colour photographs (without polarizers) of the mirror image of the clear sky reflected from the black water-dummy (glass pane underlaid by matt black cloth), patterns of the degree (d) and angle (α; measured from the local mirror meridian) of linear polarization of reflected skylight, and the area detected polarotactically as water *versus* the solar elevation (θ_s) and time (local solar time = UTC + 2 h). See Fig. 2 for further details.

computed for a perfectly black water reflector with an index of refraction (n_w) of 1.33, and we obtained practically the same results. Hence, the slightly higher index of refraction of glass makes the reflection-polarizational characteristics of glass surfaces only slightly different from those of water: the degree of linear polarization of light reflected from the glass is slightly higher and the Brewster angle of glass (θ_B=56°) is slightly wider than that of the water (θ_B=53°), for example. Thus, the conclusions drawn from the data obtained for the glass water-dummies also hold for flat water surfaces.

In Fig. 5, the left column shows the percentage, P, detected as water (polarotactic detectability) calculated for the grey and black water-dummies under clear skies as well as for the perfectly black glass (n_g=1.5) and water (n_w=1.33) reflectors as a function of the solar elevation in the blue, green and red parts of the spectrum. The polarotactic detectabilities, $P(\theta_s)$, of the perfectly black reflectors are approximately the same in all three spectral ranges, since the slight wavelength dependency of the refractive indices of glass and water can be discounted in the visible part of the spectrum. $P(\theta_s)$ of the perfectly black reflectors was calculated for the full surface of the reflectors (broken curves) as well as for the masked surface, i.e. for regions appropriate for comparative analyses (individual data points displayed with triangles). The right column in Fig. 5 shows the difference, ΔP, in the polarotactic detectability between the grey and black water-dummies as well as between the perfectly black glass and water reflectors. In Fig. 5, the following are seen:

(1) The ΔP between the perfectly black glass and water reflectors is smaller than a few percent, the maximum difference (ΔP_{max}) is 4% for $\theta_s \approx 0°$ (sun on the horizon) and ΔP=2% for higher θ_s. This also shows that the conclusions drawn from the data obtained with the glass water-dummies can also be extended to flat water surfaces.

(2) The ΔP between the full and masked surfaces of the perfectly black reflectors is smaller than 5%. From this, we conclude that the use of the masks (e.g. chequered areas in

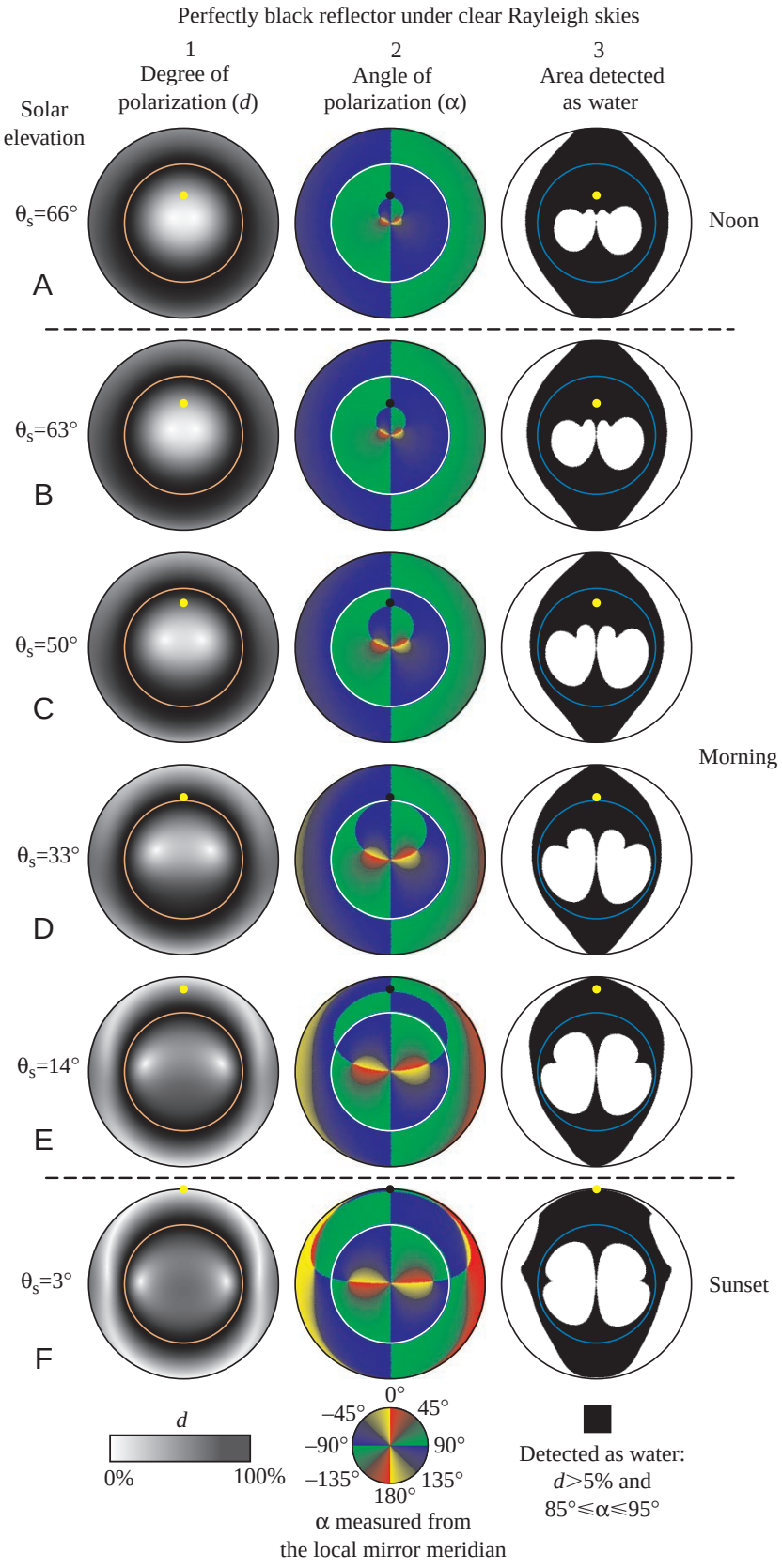

Fig. 4. Patterns of the degree (d) and angle (α; measured from the local mirror meridian) of linear polarization of reflected skylight, and the area detected polarotactically as water *versus* the solar elevation (θ_s) for a perfectly black glass (with an index of refraction of 1.5) reflector – which absorbs all penetrating light – calculated for incident single-scattered Rayleigh skylight with the use of the Fresnel formulae. The Brewster angle (56° from the nadir for glass with an index of refraction of 1.5) is represented by a circle within the circular patterns.

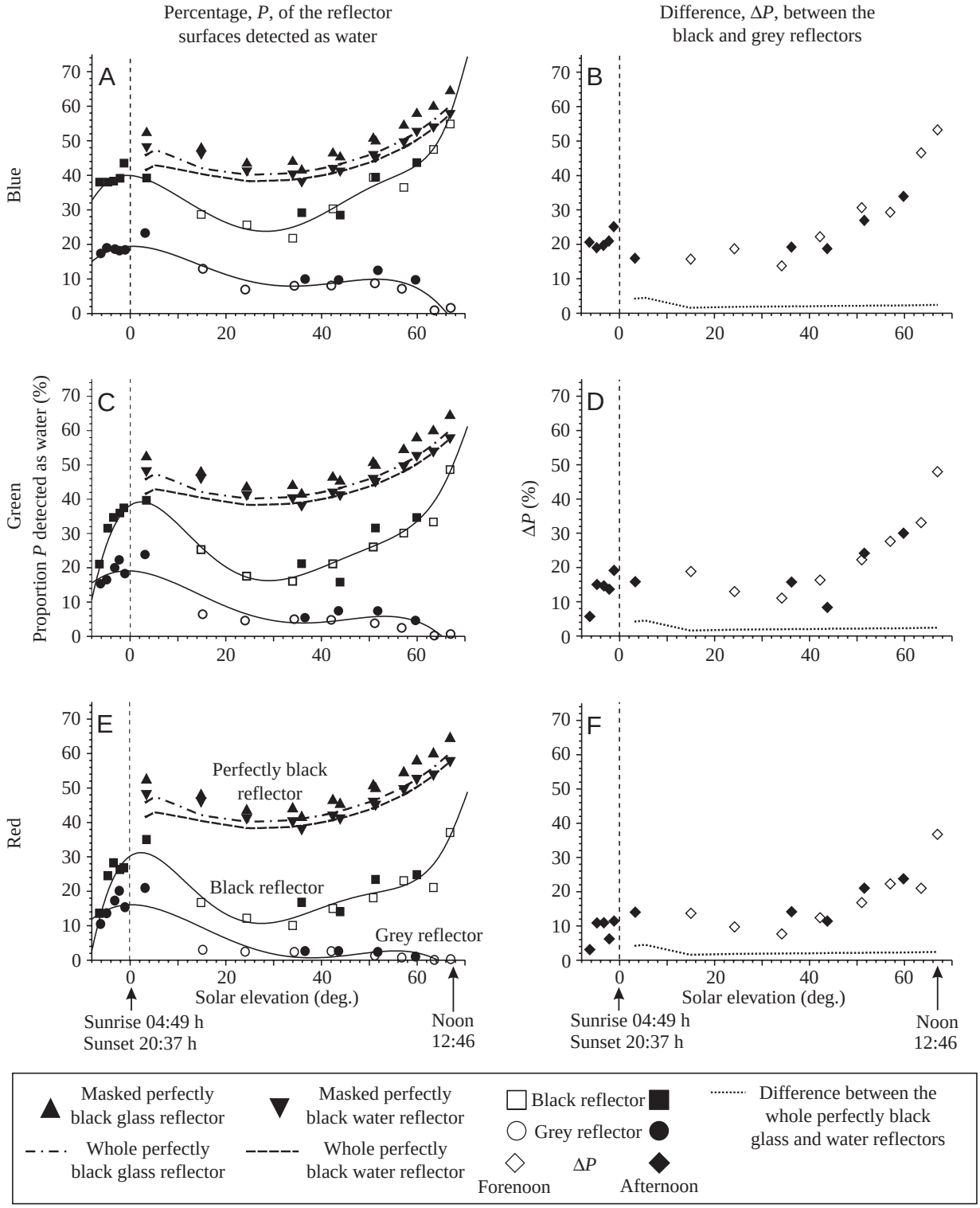

Fig. 5. Percentage, *P*, detected as water (polarotactic detectability) by an imaginary polarotactic water insect for the black (squares) and grey (dots) water-dummies (A, C, E), and difference, Δ*P*, between the black and grey water-dummies (diamonds; B, D, F) as a function of the solar elevation, θ_s, in the blue, green and red parts of the spectrum. *P* gives the proportion of the black areas in column 4 of Figs 2 and 3 relative to the entire area of the region appropriate for comparative analyses (non-chequered regions in Figs 2, 3). Data points measured in the morning and afternoon are depicted as empty and filled squares/dots/diamonds, respectively. The black continuous curves (polinomials) are fitted to these data points by the method of least squares. The dashed/dashed-dotted $P(\theta_s)$ curves are computed for the full area of a perfectly black glass (index of refraction = 1.5) and water (1.33) reflector absorbing all penetrating light. Triangles show the *P*-values calculated for the perfectly black glass and water reflectors within the regions of the field of view appropriate for comparative analyses (non-chequered regions in the *d*- and α-patterns of Figs 2, 3).

Figs 2, 3) in comparative analyses does not change significantly the *P*-values calculated for different θ_s and for the two water-dummies and does not affect our conclusions drawn from the remaining parts of the measured reflection-polarization patterns of the water-dummies.

(3) At $\theta_s \approx 0°$ (sun on the horizon), *P* has an absolute maximum for the grey water-dummy and has a local maximum for the black dummy in all three spectral ranges. Thus, in the visible part of the spectrum, polarotactic detection of brighter water bodies is easiest when the sun is approximately at the horizon. The $P(\theta_s)$ of the black water-dummy has a local minimum at $\theta_s \approx 30°$ in all three spectral ranges. For higher solar elevations, $P(\theta_s)$ of the black dummy is as high as, or even higher than, that at $\theta_s \approx 0°$. Hence, in the visible part of the spectrum, polarotactic detection of dark water bodies is easiest when the sun is either approximately at the horizon or near the zenith.

(4) The *P* of the grey water-dummy is significantly smaller throughout the day than that of the black dummy for all three spectral ranges (Mann–Whitney test, $P<0.001$). The ΔP between the grey and black water-dummies is minimal at low solar elevations in all three parts of the spectrum.

We obtained practically the same results for partly clouded skies.

Discussion

The reflection-polarizational characteristics of water surfaces depend on the illumination conditions, material composition of the bottom, dissolved organic materials, angle of view measured from the nadir and the direction of observation relative to the sun. Aquatic insects can identify their water habitat by perceiving the partial linear polarization of light reflected from the water surface if the degree of linear polarization is high enough and the direction of polarization approximates the horizontal. These two criteria are satisfied predominantly viewing towards the Brewster zone, which is continuous throughout the day for dark water bodies (Figs 3, 4), but for bright waters this is true only towards the sun and antisun and at the time of sunrise and sunset (Fig. 2). During the day, the polarotactic detectability *P* is so low for bright water bodies (Fig. 2) that water insects can easily overlook them. At bright water surfaces, both the shape and the direction of the regions suitable for polarotactic water detection change considerably with the varying solar elevation (column 4 in Figs 2, 3). Therefore, bright aquatic habitats can be recognised polarotactically only from certain directions of view with respect to the sun.

If the polarization of light reflected from water is analyzed in the whole lower hemisphere of the visual field of a flying and water-seeking imaginary polarotactic insect, *P* is proportional to the chance of a water body being recognized as water in the optical environment. Thus, in the visible part of the spectrum, polarotactic water detection is easiest in the sunrise and sunset periods, when the reflection-polarizational characteristics of dark and bright waters are most similar, the *P* of bright or dark waters is maximal and the risk that a polarotactic insect will be unable to recognize the surface of a water body is minimal. This conclusion is also valid for a visual field of the ventral polarization-sensitive eye region of water insects, which may be narrower than the whole lower hemisphere because the areas detected as water are centred at or near the Brewster angle (see column 4 of Figs 2, 3 and column 3 of Fig. 4).

We used $d_{tr}=5\%$ and $|\Delta\alpha_{tr}|=5°$ as the thresholds of the degree and angle of linear polarization for our imaginary polarotactic insect; these are characteristic of the highly polarization-sensitive blue receptors in the specialized dorsal rim area of the compound eye in the field cricket *Gryllus campestris* (Labhart, 1980). Since, in insects associated with water, the values of d_{tr} and $\Delta\alpha_{tr}$ of polarization sensitivity are unknown, and they could be species-specific, we set these values arbitrarily. However, we also computed how the polarotactic detectability of the water-dummies depends on these thresholds. We found that by increasing d_{tr}, *P* decreases monotonically, and the increase of $\Delta\alpha_{tr}$ results in the monotonous increase of *P*. Since there were no sudden changes, local extrema, breaking points or plateaus in the $P(d_{tr})$ and $P(\Delta\alpha_{tr})$ curves, we could not establish any criterion for a threshold value that could be preferred. This fact has the important consequence that the values of these two thresholds can indeed be chosen arbitrarily, and the actual choice concerns neither the relative values of *P* calculated for different θ_s nor the conclusions drawn from them. Thus, the arbitrary use of $d_{tr}=5\%$ and $|\Delta\alpha_{tr}|=5°$ is not a serious restriction.

Under clear skies at a given θ_s, the reflection-polarizational characteristics of the water-dummies as well as real water bodies depend on two components of returned light. The first component is the light reflected from the glass/water surface. The direction of polarization (e-vector direction) of this partially polarized component is usually horizontal, and if the angle of reflection is equal to the Brewster angle, it is totally polarized ($d=100\%$). The second component is the light originating from below the surface due to reflection from the underlying substratum or the bottom of the water or to backscattering from particles suspended in the water. This component is always vertically polarized due to refraction at the surface (Horváth and Pomozi, 1997). The net polarization of returned light is determined by the relative intensities of these two components. Since these two components have orthogonal directions of polarization, their superposition reduces the net degree of polarization. If the intensity of the first component is greater than that of the second, the returned light is partially linearly polarized with horizontal e-vector. When the second component is the more intense, the returned light is partially vertically polarized. Finally, if the intensities of these two components are approximately equal, the returned light is practically unpolarized.

In the ultraviolet (UV), the second component of returned light originating from below the water surface is considerably reduced in natural water bodies due to the great absorption of

UV light by the dissolved organic materials and the low UV reflectivity of the bottom (Schwind, 1995; Bernáth et al., 2002). Thus, in the UV, the majority of natural water bodies possess similar reflection-polarizational characteristics and $P(\theta_S)$ as our black water-dummy in the blue part of the spectrum (Figs 3, 5). Consequently, although we could not measure the reflection-polarization patterns of the water-dummies in the UV, our conclusions also hold for this part of the spectrum. This is important because many water insects detect water polarotactically in the UV (Schwind, 1985, 1991, 1995).

Comparing the results of our measurements performed under clear skies (Figs 2, 3, 5) with those under partly cloudy skies (data not shown), we could establish that the $P(\theta_S)$ of the water-dummies possess the same qualitative features under clear and partly cloudy skies. The light emitted by clouds is usually almost unpolarized (Können, 1985). If this nearly unpolarized cloudlight is reflected from the horizontal glass surface of the water-dummies, it always becomes partially polarized with horizontal direction of polarization. Thus, clouds can enhance the relative proportion of horizontally polarized reflected light in those regions of the reflector from which nearly vertically polarized light would be reflected if the sky were clear. Therefore, the consequence of clouds will be a slight increase in P: the more extended the cloud cover, the larger is P. Hence, under a cloudy sky, polarotactic water detection is slightly easier than under a clear sky with the same θ_S.

For $\theta_S>30°$, P increases with θ_S in the case of the black water-dummy (Fig. 5). Therefore, at high θ_S, the P of black waters could be as great as that at $\theta_S\approx0°$ (sun on the horizon). This means that at high θ_S, the polarotactic detection of dark waters can be as easy or even easier than at sunset. However, when θ_S is high (near noon), the air temperature can be much higher, the air humidity much lower and the wind speed much greater than at dusk, conditions that are disadvantageous to small-bodied water insects (1–5 mm; e.g. *Sigara* sp.). These insects possess such high surface-to-volume ratios and such thin chitinous cuticle that they can become easily dehydrated during flights of tens of minutes. Their flight can also be hindered by wind, which usually abates at sunset when direct solar radiation quickly decreases to zero (Landin and Stark, 1973). Consequently, only larger-bodied water-seeking polarotactic insects could take advantage of the high P of dark waters at high θ_S. This may be the reason why large- or medium-bodied (1–5 cm) aquatic insects (e.g. *Dytiscidae, Hydrophilidae, Notonectidae*) are attracted to horizontal black plastic sheets used in agriculture not only at dusk but also at noon (Bernáth et al., 2001a,b). These beetles can also fly for a few hours during daytime at a higher temperature and a lower air humidity due to their larger size, smaller surface-to-volume ratio and thick sclerotized cuticle, which slows down the dangerous dehydration of the body.

Schwind (1991, 1995) used quite similar water-dummies (composed of glass panes underlaid by different substrata) in his multiple-choice field experiments to our dummies. He also assumed that these dummies can imitate the reflection-polarizational and spectral characteristics of real water surfaces.

This work was supported by a 14-month Humboldt Research Fellowship from the German Alexander von Humboldt Foundation and by a three-year István Széchenyi scholarship from the Hungarian Ministry of Education to G. Horváth. We are grateful to Prof. Rüdiger Wehner (Zoological Institute, University of Zurich, Switzerland), who lent his Nikon-Nikkor fisheye lens for our polarimetric measurements. Many thanks to Sándor Hopp and Endre Berecz (Mechanical Workshop, Eötvös University, Budapest) for constructing the polarimeter holder. Thanks are also due to Prof. Rudolf Schwind (Institute of Zoology, University of Regensburg, Germany) for reading and commenting on an earlier version of the manuscript, and to Prof. Béla Böddi (Department of Plant Anatomy, Eötvös University, Budapest) for measuring the relative reflectivity of our water-dummies (Fig. 1C). The constructive comments of two anonymous referees are acknowledged.

References

Bernáth, B., Szedenics, G., Molnár, G. and Horváth, G. (2001a). Visual ecological impact of a peculiar oil lake on the avifauna: dual choice field experiments with water-seeking birds using huge shiny black and white plastic sheets. *Arch. Nat. Conserv. Landsc. Res.* **40**, 1-28.

Bernáth, B., Szedenics, G., Kriska, G. and Horváth, G. (2001b). Visual ecological impact of “shiny black anthropogenic products” on aquatic insects: oil reservoirs and plastic sheets as polarized traps for insects associated with water. *Arch. Nat. Conserv. Landsc. Res.* **40**, 87-107.

Bernáth, B., Szedenics, G., Wildermuth, H. and Horváth, G. (2002). How can dragonflies discern bright and dark waters from a distance? The degree of polarization of reflected light as a possible cue for dragonfly habitat selection. *Freshw. Biol.* **47**, 1707-1719.

Danilevskii, A. S. (1965). *Photoperiodism and Seasonal Development of Insects*. Edinburgh, London: Oliver and Boyd.

Danthanarayana, W. (ed.) (1986). *Insect Flight: Dispersal and Migration*. Berlin, Heidelberg, New York: Springer.

Fernando, C. H. and Galbraith, D. (1973). Seasonality and dynamics of aquatic insects colonizing small habitats. *Verhandl. Int. Verein Limnol.* **18**, 1564-1575.

Gál, J., Horváth, G. and Meyer-Rochow, V. B. (2001a). Measurement of the reflection-polarization pattern of the flat water surface under a clear sky at sunset. *Rem. Sens. Environ.* **76**, 103-111.

Gál, J., Horváth, G. and Meyer-Rochow, V. B. (2001b). Polarization patterns of the summer sky and its neutral points measured by full-sky imaging polarimetry in Finnish Lappland north of the Artic Circle. *Proc. R. Soc. Lond. A* **457**, 1385-1399.

Horváth, G. (1995). Reflection-polarization patterns at flat water surfaces and their relevance for insect polarization vision. *J. Theor. Biol.* **175**, 27-37.

Horváth, G., Barta, A., Gál, J., Suhai, B. and Haiman, O. (2002). Ground-based full-sky imaging polarimetry of rapidly changing skies and its use for polarimetric cloud detection. *Appl. Opt.* **41**, 543-559.

Horváth, G., Bernáth, B. and Molnár, G. (1998). Dragonflies find crude oil visually more attractive than water: multiple-choice experiments on dragonfly polarotaxis. *Naturwissenschaften* **85**, 292-297.

Horváth, G., Gál, J. and Wehner, R. (1997). Why are water-seeking insects not attracted by mirages? The polarization pattern of mirages. *Naturwissenschaften* **84**, 300-303 [Erratum **85**, 90].

Horváth, G. and Pomozi, I. (1997). How celestial polarization changes due to reflection from the deflector panels used in deflector loft and mirror experiments studying avian navigation. *J. Theor. Biol.* **184**, 291-300.

Horváth, G. and Varjú, D. (1997). Polarization pattern of freshwater habitats recorded by video polarimetry in red, green and blue spectral ranges and its relevance for water detection by aquatic insects. *J. Exp. Biol.* **200**, 1155-1163.

Horváth, G. and Varjú, D. (2003). *Polarized Light in Animal Vision – Polarization Patterns in Nature*. Heidelberg, Berlin, New York: Springer.
Horváth, G. and Zeil, J. (1996). Kuwait oil lakes as insect traps. *Nature* **379**, 303-304.
Johnson, G. C. (1969). *Migration and Dispersal of Insects by Flight.* London: Methuen and Co.
King, R. S. and Wrubleski, D. A. (1998). Spatial and diel availability of flying insects as potential duckling food in prairie wetlands. *Wetlands* **18**, 100-114.
Können, G. P. (1985). *Polarized Light in Nature*. Cambridge: Cambridge University Press.
Kriska, G., Horváth, G. and Andrikovics, S. (1998). Why do mayflies lay their eggs en masse on dry asphalt roads? Water-imitating polarized light reflected from asphalt attracts Ephemeroptera. *J. Exp. Biol.* **201**, 2273-2286.
Labhart, T. (1980). Specialized photoreceptors at the dorsal rim of the honeybee's compound eye: polarizational and angular sensitivity. *J. Comp. Physiol. A* **141**, 19-30.
Landin, J. (1968). Weather and diurnal periodicity of flight by *Helophorus brevipalpis* Bedel (Col. Hydrophilidae). *Opusc. Entomol.* **33**, 28-36.
Landin, J. and Stark, E. (1973). On flight thresholds for temperature and wind velocity, 24-hour flight periodicity and migration of the water beetle *Helophorus brevipalpis*. *ZOON* **Suppl. 1**, 105-114.
Popham, E. J. (1964). The migration of aquatic bugs with special reference to the Corixidae (Hemiptera Heteroptera). *Arch. Hydrobiol.* **60**, 450-496.
Schwind, R. (1985). Sehen unter und über Wasser, Sehen von Wasser. *Naturwissenschaften* **72**, 343-352.
Schwind, R. (1991). Polarization vision in water insects and insects living on a moist substrate. *J. Comp. Physiol. A* **169**, 531-540.
Schwind, R. (1995). Spectral regions in which aquatic insects see reflected polarized light. *J. Comp. Physiol. A* **177**, 439-448.
Schwind, R. and Horváth, G. (1993). Reflection-polarization pattern at water surfaces and correction of a common representation of the polarization pattern of the sky. *Naturwissenschaften* **80**, 82-83.
Wildermuth, H. (1998). Dragonflies recognize the water of rendezvous and oviposition sites by horizontally polarized light: a behavioural field test. *Naturwissenschaften* **85**, 297-302.
Zalom, F. G., Grigarick A. A. and Way, M. O. (1979). Seasonal and diel flight periodicities of rice field Hydrophilidae. *Environ. Entomol.* **8**, 938-943.
Zalom, F. G., Grigarick, A. A. and Way, M. O. (1980). Diel flight periodicities of some Dytiscidae (Coleoptera) associated with California rice paddies. *Ecol. Entomol.* **5**, 183-187.